STEM CELLS AND DEVELOPMENT
Volume 21, Number 12, 2012

DOI: 10.1089/scd.2011.0605

Inhibition of Planar Cell Polarity Extends Neural Growth During Regeneration, Homeostasis, and Development

Wendy S. Beane, Ai-Sun Tseng,* Junji Morokuma,* Joan M. Lemire, and Michael Levin

The ability to stop producing or replacing cells at the appropriate time is essential, as uncontrolled growth can lead to loss of function and even cancer. Tightly regulated mechanisms coordinate the growth of stem cell progeny with the patterning needs of the host organism. Despite the importance of proper termination during regeneration, cell turnover, and embryonic development, very little is known about how tissues determine when patterning is complete during these processes. Using planarian flatworms, we show that the planar cell polarity (PCP) pathway is required to stop the growth of neural tissue. Although traditionally studied as regulators of tissue polarity, we found that loss of the PCP genes *Vangl2*, *DAAM1*, and *ROCK* by RNA interference (individually or together) resulted in supernumerary eyes and excess optical neurons in intact planarians, while regenerating planarians had continued hyperplasia throughout the nervous system long after controls ceased new growth. This failure to terminate growth suggests that neural tissues use PCP as a readout of patterning, highlighting a potential role for intact PCP as a signal to stem and progenitor cells to halt neuronal growth when patterning is finished. Moreover, we found this mechanism to be conserved in vertebrates. Loss of Vangl2 during normal development, as well as during *Xenopus* tadpole tail regeneration, also leads to the production of excess neural tissue. This evolutionarily conserved function of PCP represents a tractable new approach for controlling the growth of nerves.

Introduction

Tissue growth is a central component of many processes, including embryonic development, homeostatic renewal (such as the replacement of skin or blood cells), and regeneration (following injury or disease). During tissue growth, an organism must determine what structures are needed or missing, what final pattern any new tissues should take, and importantly—when to stop growing. Regulated proliferation, whereby new tissue growth has a set ending point, is essential to maintaining overall body patterning and functionality. Even though unwanted, continual growth of cells and tissues can have dire consequences (as when uncontrolled proliferation leads to cancer), very little is known about how new growth is halted during normal biological processes. Understanding how to stop tissue growth will be critical for the advancement of many clinical therapies, especially in regenerative medicine where the goal is to correctly restore lost organs and limbs while ensuring that both proportion and function are maintained.

We used the planarian model system, popular for regeneration studies due to a robust ability to regenerate any body part [1], to begin elucidating the sensor that terminates growth. An accessible population of adult stem cells [2] makes planaria an excellent in vivo system for studying the mechanisms by which adult stem cells direct large-scale morphologies. During tissue growth, stem and progenitor cells must be integrated with surrounding tissues, suggesting there exists a mechanism that directs stem cells to proliferate only the necessary structures—stem cells and/or new tissues must sense when that growth is complete. We decided to investigate whether the versatile planar cell polarity (PCP) pathway (Fig. 1A) might function as part of this termination sensor. Originally identified as a determinant of epithelial tissue polarity from the asymmetrical localization of pathway proteins within single cells [3], PCP also regulates cell size, proliferation, and migration [4–6], as well as neuronal morphogenesis and the migration of both neurons and neural progenitor cells during development [7–10]. In planarian flatworms, the conserved PCP pathway is known to regulate epithelial polarity as in other organisms [11]. We hypothesized that PCP, which coordinates individual cell behaviors into tissue-wide organization, could be involved in neuronal growth regulation signals on an organism-wide scale.

Our investigations looked specifically at growth termination of the nervous system, uncovering a role for PCP in terminating the growth of neural tissues during planarian regeneration and homeostatic cell turnover. The central

Biology Department and Tufts Center for Regenerative and Developmental Biology, Tufts University, Medford, Massachusetts.
*These authors contributed equally to this work.

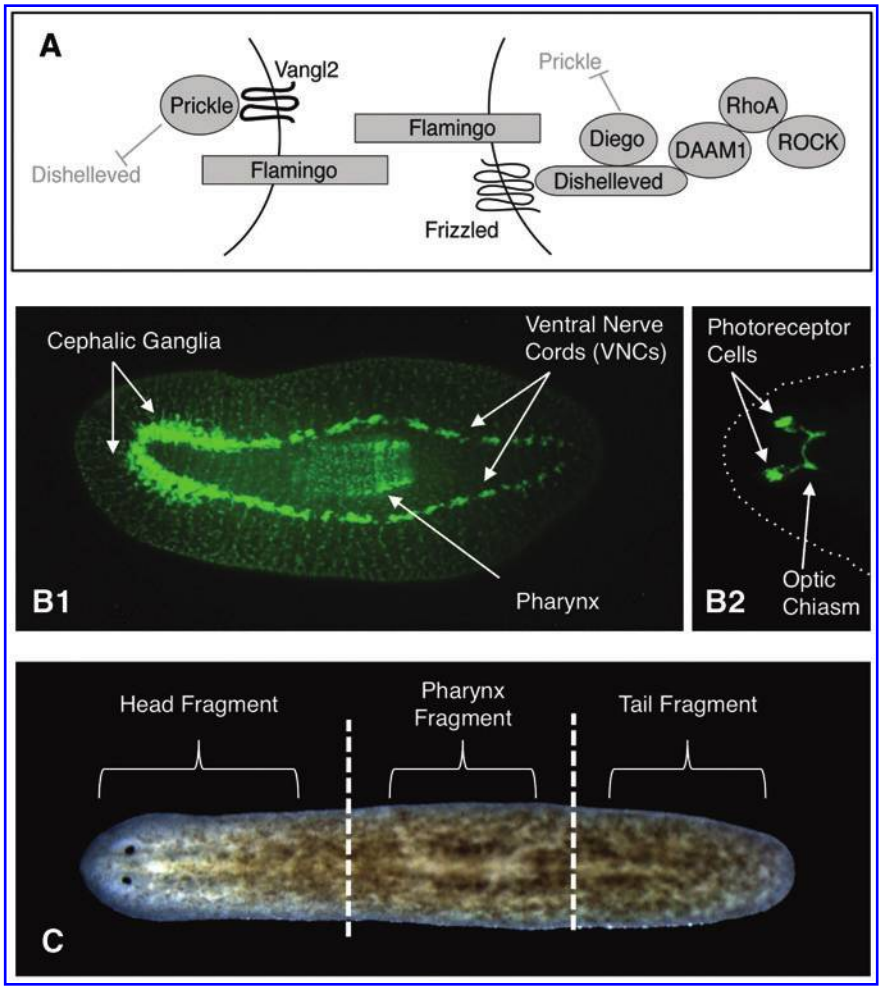

FIG. 1. **(A)** Diagram of the planar cell polarity pathway, illustrating interaction between 2 cells. **(B)** Diagram of the planarian nervous system. *Dotted line* in **(B2)** represents outline of worm. **(C)** Diagram of cuts (*dotted lines* represent amputation planes). Anterior is left. Color images available online at www.liebertonline.com/scd

nervous system (CNS) of freshwater planaria consists of a bilobed cephalic ganglia (brain) and 2 ventral nerve cords (VNCs) that run the length of the animal (Fig. 1B1), an optic chiasm connected to photoreceptor cells (Fig. 1B2), as well as an intricate network of commissural and sensory neurons throughout the periphery [12,13]. In addition, planaria possess most of the same neurotransmitters found in vertebrates [14–16], making them an excellent model system for understanding neural patterning [17]. Our data show that loss of PCP through gene silencing in planarians resulted in continued neural hyperplasia for at least 6 weeks after the normal 2-week regeneration period, as well as causing the formation of excess neurons in intact planarians during normal cell turnover. Further, PCP inhibition in *Xenopus* tadpoles revealed that PCP-mediated regulation of neural growth during regeneration is conserved in vertebrates, while demonstrating that PCP also limits neuronal growth during embryogenesis. Together, our results suggest that the mechanism of PCP signaling acts to restrict neural growth during regeneration, homeostasis, and development.

Methods and Materials

Cloning

Homologs to Vang-like 2 (*Vangl2/Van Gogh/Strabismus*), Dishevelled-associated activator of morphogenesis 1 (*DAAM1*), and Rho-associated kinase (*ROCK*) were used to identify the *Schmidtea mediterranea* counterparts in the Genome Database [18], and the planarian genes were generated by common protocols. For details, see Supplementary Materials and Methods (Supplementary Data available online at www.liebertonline.com/scd). GenBank accession numbers: *Smed-DAAM1* (JN100092), *Smed-ROCK* (JN100093), and *Smed-vang-1* (Vangl2) (JN100094).

Colony care and amputations

The CIW4 clonal line of asexual *S. mediterranea* was used and maintained as previously described [19]. Worms 4–7 mm long were starved for ≥1 week prior to use. Details on care and amputations are provided in Supplementary Materials and Methods.

In situ hybridization

Worms for whole-mount in situ hybridization were formalin fixed, and in situs were performed as described by Pearson et al. [20]. Use of this protocol may explain the differences between our *Smed-vang-1* staining and that previously reported [11]—which used a different protocol and did not observe intestinal upregulation (see Supplementary Fig. S3 for probe controls). Probes: *Piwi-1* [21]; *NB.21.11.e* [22]; *sFRP-1* and *WntP-2/Wnt11-5*, kind gifts of P. Reddien [23]; and *Cintillo* [24].

Immunofluorescence

Worms were fixed in Carnoy's fixative and antibody stained by common protocols. For details, see Supplementary Materials and Methods. Primary antibodies: anti-phosphorylated histone H3, 1:250; anti-arrestin, 1:10,000 (kind gift from K. Watanabe); and anti-synapsin, 1:50 (Developmental Studies Hybridoma Bank). Secondary antibodies: goat anti-mouse Alexa488, 1:400 (Sigma); or for H3P, a horseradish peroxidase (HRP)-conjugated anti-Rabbit with TSA-Alexa568 anti-HRP (Molecular Probes). For excess photoreceptor counts, discrete areas of ectopic anti-arrestin staining were scored (eg, see yellow arrows in arrestin staining images).

RNA interference

For RNA interference (RNAi) experiments, dsRNA was generated and injected as described by Oviedo et al. [25]. For details, see Supplementary Materials and Methods. Combination *PCP-Cocktail-RNAi* was made by injecting with equal parts of *DAAM1*, *ROCK*, and *Vang-1 RNAi*. Control injections were with either *PC2-RNAi* or *VENUS-GFP RNAi*.

Image collection and statistics

Images were collected using either a Nikon SMZ1500 microscope with a Retiga 2000R camera (Q-Imaging) and Q-Capture imaging software, or an Olympus BX61 compound microscope with a Hamamatsu Orca AG CCD camera and IP Labs or MetaMorph imaging software. Adobe Photoshop was used to orient and scale images and improve contrast. Data were neither added nor subtracted; original images available upon request. Microsoft Excel was used to calculate Student's *t*-test (2-tailed distribution, 2 independent samples, unequal variance).

Xenopus experiments

Xenopus laevis larvae were cultured via approved protocols (Institutional Animal Care and Use Committee, #M2008-08). Four-cell-stage embryos were injected into 2 of 4 cells using 1 mM Vangl2 morpholino (*Vangl2-MO*; Gene Tools). The *Vangl2-MO* [26,27] is tagged with flourescein, and its presence in stage-40 tail tissues was identified by fluorescence. For tail regeneration, tails with good flourescein expression at stages 40–41 were amputated at the midpoint between the anus and the tip. Tadpoles were cultured in 0.1 × Marc's modified Ringers at 22°C for 10 days. *Xenopus* embryos were fixed overnight in 100 mM MOPS at pH 7.4, 2 mM EGTA, 1 mM MgSO4, 3.7% v/v formaldehyde [28] and processed for immunohistochemistry using standard protocols. Antiacetylated tubulin (Sigma) at 1:1,000 and goat anti-mouse Alexa555 (Molecular Probes) at 1:500 were used to visualize the nervous system.

Results and Discussion

Cloning planarian PCP genes

Searching the *S. mediterranea* genome [18] by sequence homology, we identified and cloned full-length planarian homologs for Van Gogh 2 (Vangl2, recently named *Smed-vang-1* in *11*), Rho-associated kinase (*Smed-ROCK*, Supplementary Fig. S1), and Dishevelled-associated activator of morphogenesis 1 (*Smed-DAAM1*, Supplementary Fig. S2). When analyzed by in situ hybridization in untreated, intact planaria, these genes were expressed throughout the worm, with some upregulation in the gastrovascular tract and anterior neural tissues (Fig. 2 and Supplementary Fig. S3). Analyses during regeneration showed that all 3 genes were upregulated in both the anterior and posterior blastemas. In particular, both *Vang-1* and *DAAM1* appeared to be slightly upregulated in the brain primordia at day 3 of regeneration (Fig. 2, red arrows). This upregulation was gone by 7 days, although all 3 genes continued to be expressed in both blastemas throughout regeneration (Supplementary Fig. S3).

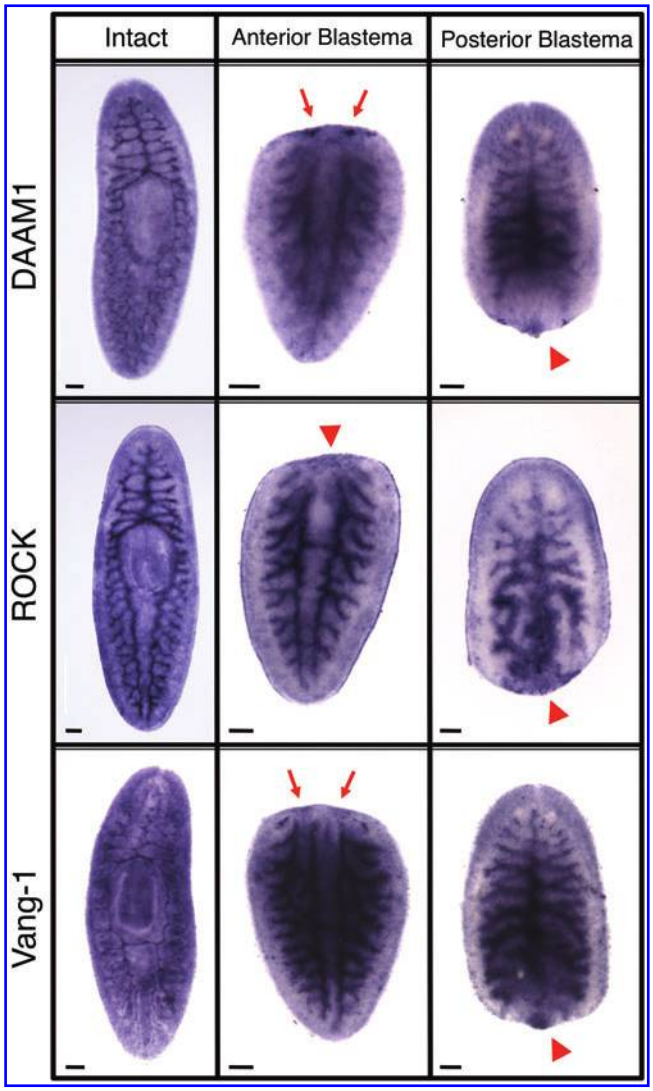

FIG. 2. Planarian planar cell polarity (PCP) genes. In situ hybridization patterns in intact (whole) and regenerating (at day 3 post-amputation) bisected planaria. Vangl2 (*Smed-vang-1*), Rho-associated kinase (*Smed-ROCK*), and Dishevelled-associated activator of morphogenesis 1 (*Smed-DAAM1*). *Arrowheads* indicate expression in the blastema. *Arrows* indicate expression in brain primordia. Anterior is up. Scale bars: 100 μm. Color images available online at www.liebertonline.com/scd

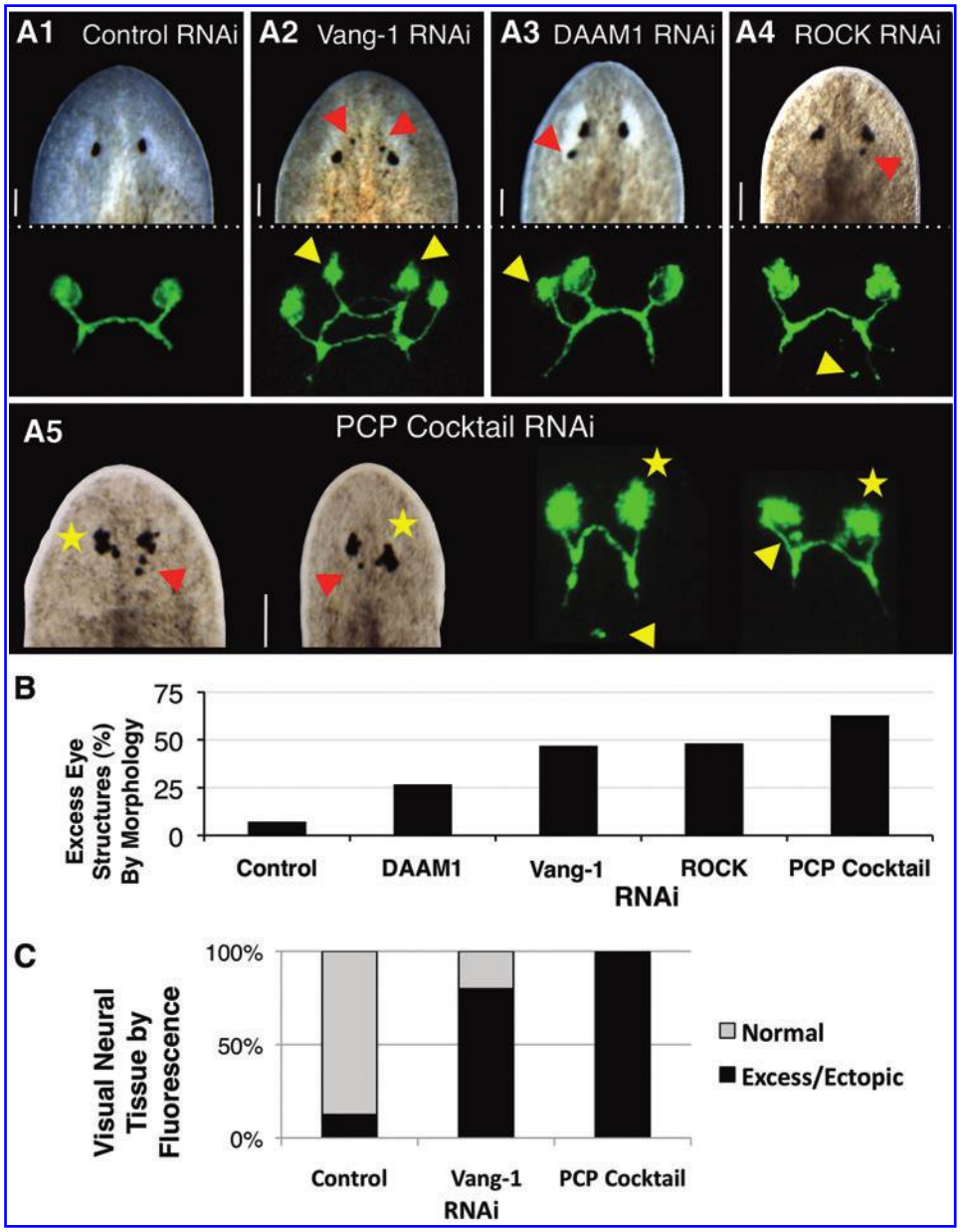

FIG. 3. PCP regulates eye innervation and visual neuron formation during regeneration. **(A)** Eye morphology in PCP-inhibited regenerates at 8 weeks. PCP Cocktail RNA interference (RNAi) is a combination of *Vang-1*, *ROCK*, and *DAAM1* RNAi. Representative antiarrestin (VC1) antibody staining of visual neurons in *green*. *Arrowheads*: excess pigment cells (*red*) and excess photoreceptors (*yellow*). *Asterisks*: "cauliflower" phenotype. Anterior is up. Scale bars: 100 μm. **(B)** Percentage of supernumerary eye structures (by morphology) in PCP-inhibited head and tail regenerates at 8 weeks ($n > 27$). **(C)** Percentage of PCP-inhibited head and tail regenerates with excess and/or ectopic visual neural tissue (by immunofluorescence) at 8 weeks ($n > 8$). Color images available online at www.liebertonline.com/scd

Loss of PCP results in excess visual neuron growth during planarian regeneration

Since new tissue growth is perhaps most easily assessed as part of blastema formation, we began by investigating the role of PCP during regeneration. We used RNAi to silence *Vang-1*, *DAAM1*, and *ROCK* in regenerating head, pharynx, and tail fragments (Fig. 1C), and uncovered a role for PCP specifically in restricting the growth of the regenerating nervous system. As regeneration in planarians is typically scored at 2 weeks post-amputation, we assessed animals at 8 weeks post-amputation to identify possible effects from continued regenerative growth. The first phenotype observed was an increase in eye structures following PCP inhibition. During regeneration, eye structures first become visible ~5–7 days following decapitation. Although it usually occurs normally, eye regeneration in planaria is somewhat labile; even during normal asexual fissioning, a 1% occurrence of supernumerary eye regeneration has been reported [29]. When untreated controls are experimentally amputated, the appearance of excess eye structures (such as pigment cells) during regeneration can be as high as 6.7% ($n = 30$).

We found that regenerates injected with RNAi targeting individual PCP pathway members possessed excess eyes and supernumerary eye structures (such as pigment cells) in an average of 31.1% of animals (Figs. 3A2 and 4), versus only 7.2% when control RNAi was injected (Fig. 3A1). Specific counts of pigment cells in *Smed-vang-1(RNAi)*-injected animals at 8 weeks of regeneration revealed an average of 1.16 extra pigment cells per animal (red arrows in Fig. 3A), as compared with only 0.1 extra pigment cells in controls ($n > 18$, $P < 0.001$). Inhibition of single PCP genes by RNAi also resulted in several eye patterning defects, including abnormal eye alignment and asymmetric eye size and orientation (Supplementary Fig. S4), consistent with PCP's known role in patterning. To maximize the effects of PCP inhibition, RNAi targeting *Vang-1*, *DAAM1*, and *ROCK* was combined (*PCP Cocktail RNAi*), which resulted in up to a 2-

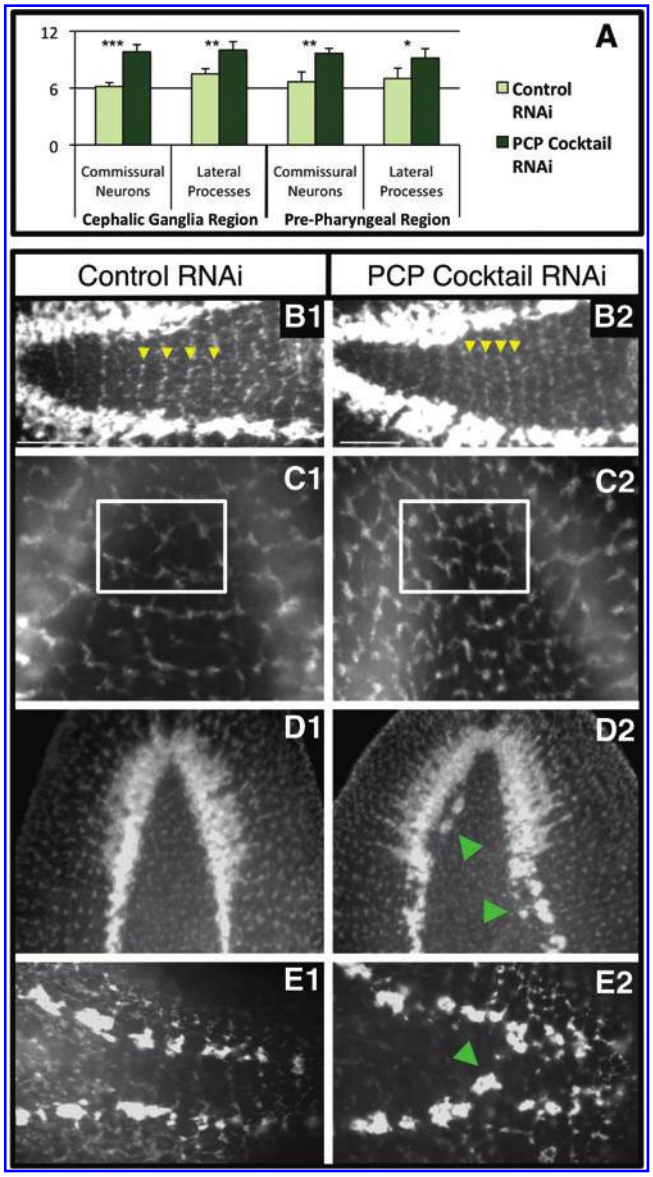

FIG. 4. Loss of PCP results in neural hyperplasia. PCP regulates regeneration of both the central and peripheral nervous systems. **(A)** PCP inhibition results in increased numbers of both transverse commissures between the ventral nerve cords (VNCs) and associated lateral processes. Anti-synapsin (3C11)–labeled neurons within a 200 μm area were counted in 2 separate regions at 2 weeks in pharynx regenerates ($n=6$). ***$P<0.0001$, **$P<0.001$, *$P<0.01$. *Error bars* denote standard deviation. Scale bars: 100 μm. **(B–E)** Anti-synapsin labeling at 2 weeks in pharynx regenerates ($n>24$). **(B)** Transverse commissures (*yellow arrows*) in the head and prepharyngeal regions. **(C)** Anterior dorsal submuscular nerve complex. Insets highlight the differences in the neural plexus. **(D)** Anterior central nervous system (bilobed cephalic ganglia and anterior VNCs). **(E)** Posterior VNCs. *Green arrows*: ectopic neurons. Anterior is up, except for **(B, E)** where anterior is left. Color images available online at www.liebertonline.com/scd

fold increase in phenotypic effects (Fig. 3B). In particular, this combination increased visual cell regeneration, leading to a "cauliflower" phenotype where numerous excess pigment cells were overlaid (Fig. 3A5 and Supplementary Fig. S4). This demonstrates that the PCP pathway regulates eye regeneration, suggesting a role for PCP in stopping the formation of visual neurons as well as in neural patterning.

To corroborate our morphological observations, we examined the placement of optic nerves using a visual-neuron-specific marker that recognizes planarian photoreceptor cells (Fig. 3A, C). By 8 weeks of regeneration (6 weeks after regeneration is typically considered complete) we observed both extra photoreceptors and optic neuronal projections following RNAi injection for each of the 3 genes in regenerating head and tail fragments. Counts of *Smed-vang-1 (RNAi)*-injected animals revealed an average of 1.7 discrete areas of excess photoreceptor staining per animal (yellow arrows in Fig. 3A) when *Vang-1* was inhibited, as compared with 0.3 in controls ($n\geq 20$, $P<0.001$). The increase in visual neurons detected by immunofluorescence when single PCP genes were inhibited was much more penetrant than the corresponding increase in eye structures detected by morphology alone (81% on average, vs. 31.1%).

Strikingly, injection of the combination *PCP Cocktail RNAi*, while producing similar phenotypes to individual RNAi injections, increased the incidence of excess optic neural tissue to 100% of tested regenerates (Fig. 3C). Additionally, ectopic photoreceptors (normally anterior to the optic chiasm) were seen atypically in more posterior tissues (yellow arrows in Fig. 3A5), although none was ever observed outside of the tissues anterior to the pharynx. Analyses of anterior and posterior molecular markers confirmed that PCP inhibition had no effect on the anterior-posterior polarity of the fragments (Supplementary Fig. S5). The occurrence of excess photoreceptors following inhibition of PCP genes (both individually and together) is consistent with excess optic neural growth following RNAi to another PCP pathway member, RhoA, in a different planarian species [30]. Our data reveal that multiple visual cell types (both pigment cells and photoreceptors) were affected by PCP inhibition. This implicates PCP signaling in regulating the formation of new neurons in planarians, rather than merely augmenting axon regeneration. Together, these data suggest that PCP regulates optic neuronal replacement during regeneration, controlling both the extent and patterning of visual innervation.

PCP is required to terminate visual neuron growth during planarian homeostasis

Morphostasis of adult bodies requires continual replacement of aging tissues. Because neural growth occurs not just during regeneration, but also during homeostatic cell renewal, we next looked at eye morphology in intact worms (not undergoing regeneration) following PCP inhibition. Although excess eye structures never occurred in control worms ($n=9$), supernumerary eye structures began to appear 2–4 weeks after injection of *Smed-vang-1(RNAi)* (Supplementary Fig. S6A). At 8 weeks post-injection, *Smed-vang-1(RNAi)* in intact worms resulted in 29.2% of animals with supernumerary eye structures ($n=26$). The delayed timing for the onset of excess neural tissue formation in intact PCP-inhibited worms is consistent with a role for PCP during cell turnover in the planarian nervous system, although it does not rule out cell differentiation effects. These data suggest that the PCP pathway is required to inhibit neural growth during homeostasis, as well as during regeneration.

Loss of PCP leads to neural hyperplasia throughout the planarian nervous system

To determine whether PCP's role in neuron renewal was limited to visual nerves, we examined the entire planarian nervous system following PCP silencing. We continued our analyses using the combination *PCP Cocktail RNAi*, since the phenotypic penetrance of RNAi to individual genes was suboptimal. We found that *PCP Cocktail RNAi* in regenerating pharynx fragments resulted in increased nerve induction and disrupted neural patterning throughout the animal when visualized by a pan-neural maker (Fig. 4). To identify regeneration-specific phenotypes (by reducing the effects from PCP regulation of neural homeostasis), we injected RNAi following amputation and scored at 2 weeks post-amputation when neural regeneration is first considered complete. Analyses of the commissural neurons that connect the brain and 2 VNCs revealed that following injection of *PCP Cocktail RNAi* there was a 51.9% increase in the number of transverse commissures, as well as a 32.1% increase in the number of associated lateral processes when compared with controls (Fig. 4A, B). These data demonstrate that the presence of excess neuronal growth following PCP inhibition is not limited to the visual neurons but extends throughout the planarian nervous system. We also observed additional neuronal phenotypes in *PCP Cocktail RNAi*–injected worms. In the peripheral nervous system, the dorsal submuscular nerve plexus was mispatterned, with dense and irregularly spaced neurons consistent with increased nerve regeneration (Fig. 4C). The CNS exhibited patterning defects as well, with excess and/or ectopic neurons extending from the cephalic ganglia (Fig. 4D) (without an apparent increase in the overall size of the brain region) and along the VNCs (Fig. 4D, E). Together, excess and/or ectopic CNS and peripheral neural tissue occurred in 81.5% of *PCP Cocktail RNAi*–injected regenerates (vs. 8.3% with control RNAi). Together, these data suggest that PCP regulates replacement of the entire nervous system during regeneration.

Loss of PCP results in increased proliferation and stem cell progeny

Our data demonstrate that PCP regulates neuronal growth, but this could be the result of disrupted neuronal patterning rather than a failure to terminate growth. If increased nerve formation was due to initial mispatterning, then we would expect the number of ectopic nerves to stay the same after regeneration was completed. However, if excess neural tissue was the result of a failure to halt regenerative growth, we would expect to see continued nerve formation over time. This last hypothesis was consistent with our observations of eye regrowth in *PCP Cocktail RNAi*–injected worms, where excess eye structures appeared to gradually accumulate rather than arise immediately (Fig. 5A). To distinguish between the 2 hypotheses, regenerating *Vang-1*-inhibited worms were followed over the course of 8 weeks. RNAi to *Smed-vang-1* alone was used because its incomplete penetrance would highlight any increases in eye growth. When the same worms were examined visually every 2 weeks, we found that the incidence of excess eye structures doubled within 2 months, with the largest increase between 6 and 8 weeks (Fig. 5B1). The initial incidence of excess eye structures at 2 weeks of regeneration was comparable to our previously observed incidence at 8 weeks as a result of homeostasis (29% for each). However, the much higher incidence of excess eye structures by 8 weeks of regeneration (57%), along with the continued formation of new eye tissue over the course of the trial, indicates that these results are regeneration specific. The data suggest that loss of PCP results in more than disrupted neuronal patterning, but that PCP genes play a role in halting neuronal regeneration.

This continual maintenance of regenerative growth implies that there was similarly extended mitotic activity in PCP-inhibited worms. Planarian regeneration is accompanied by a marked mitotic increase [31], leading to new tissue formation and patterning. When we examined mitotic activity by phosphorylated histone-3 labeling, we observed that increased mitosis was still present at 8 weeks of regeneration in *Vang-1*-inhibited regenerates (Fig. 5B3), which was not seen in control regenerates (Fig. 5B2). This is consistent with our observations that neural growth continues over time when PCP is inhibited, and suggests that PCP is required for regeneration-mediated proliferation to cease.

In planarians, the only mitotically active cells are a large population of pluripotent adult stem cells (neoblasts) responsible for replacing all lost or damaged cells [32,33]. Increased mitotic activity following PCP inhibition could be the result of increased numbers of neoblasts. However, when visualized by *Smed-piwi-1* staining, we did not observe an increase in the neoblast population in *PCP Cocktail RNAi*–injected regenerates (Fig. 5C). Alternatively, sustained mitosis could be the result of an increase in stem cell progeny produced from the normal neoblast population. Using a marker of early neoblast descendents, *Smed-NB.21.11e* [22], we observed a modest increase at 8 weeks post-amputation in neoblast progeny after PCP inhibition (Fig. 5D), consistent with increased neural growth throughout the entire planarian nervous system. While our data are indicative of increased neuron numbers due to more proliferative cycles (resulting in additional stem cell progeny), it does not rule out the possibility that PCP inhibition also influences stem cell fate changes. If such fate changes do exist, they likely involve the new stem cell progeny, rather than altering the differentiation of existing stem cells, as our analysis revealed no evidence of defects that would result from diverting neoblasts from making other necessary tissues. However, detailed investigation of other organ systems in PCP-inhibited regenerates will be required to determine whether or not stem cell fates are being switched to neural at the expense of another cell type. It is noteworthy that at 8 weeks of regeneration overall body morphology in PCP-inhibited worms was indistinguishable from controls—PCP inhibition did not result in either larger/overgrown or smaller/undersized worms (Supplementary Fig. S6B). This suggests at a minimum that the master regulator that maintains planarian body shape over time (allometric scaling) is still functional even when PCP is disrupted.

PCP restricts neural growth during vertebrate regeneration and development

The data suggest that PCP is required to limit neural tissue growth during both homeostasis and regeneration in

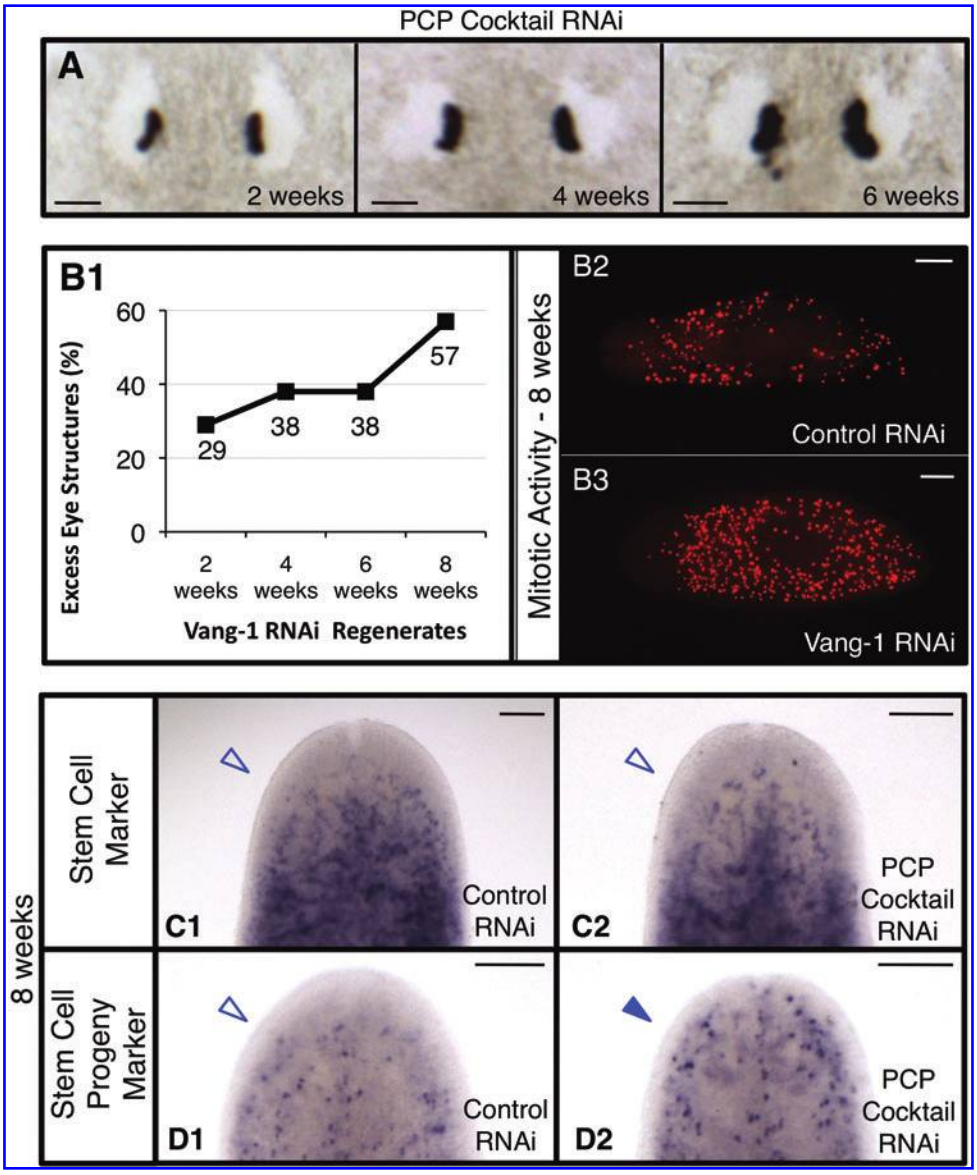

FIG. 5. PCP inhibits stem-cell-mediated growth during regeneration. **(A)** Eye regeneration in a single *PCP Cocktail RNAi* regenerate followed over 6 weeks postamputation. Scale bars: 50 μm. **(B)** *Smed-vang-1*(*RNAi*) head and tail regenerates. **(B1)** Trend of supernumerary eye structures over time ($n = 45$). **(B2, B3)** Mitotic activity detected by antiphosphorylated histone H3 labeling (H3P) at 8 weeks in the same regenerates as **(B1)**. Average number of H3P-positive cells: control = 137; Vang-1 = 338 ($P < 0.001$, $n \geq 6$). Scale bars: 200 μm. **(C, D)** In situ hybridizations in 8-week pharynx regenerates following *PCP Cocktail RNAi* injection ($n \geq 5$). **(C)** Stem cell/neoblast marker *Smed-piwi-1*. Note the expression patterns are similar. **(D)** Early neoblast progeny marker *Smed-NB.21.11e*, showing a slight increase with PCP inhibition. *Open arrowheads*: normal expression. *Solid arrowhead*: increased expression. Anterior is up, except for **(B)** where anterior is left. Color images available online at www.liebertonline.com/scd

planarians. To test whether the PCP pathway also regulates neural replacement in vertebrates, we examined the effects of a *Vangl2* morpholino (*XVangl2-MO*) [26,27] during *Xenopus* tadpole tail regeneration (Fig. 6), a well-established regenerative model we have previously used to identify novel regulators of regeneration [34,35]. *Xenopus Vangl2* is upregulated in neural tissues during development and is involved in both gastrulation and neural tube closure [36,37]. Following tail amputation, *XVangl2-MO*-injected tadpoles regenerated with excess neural tissue that extended ectopically toward the tip of the new tail, corresponding to a 32.8% increase in neuronal length (Fig. 6A). This suggests that PCP-mediated termination of neural growth is conserved in *Xenopus* regeneration. Further, we found that *Vangl2* inhibition during normal tadpole development (without amputation) revealed excess neuronal growth along the flank (Fig. 6B), as well as a 20.9% increase in neuronal length toward the tip of the tail (Fig. 6C). This suggests that *Vangl2* also acts to restrict neural growth in *Xenopus* during embryonic development. The data implicate a conserved role for PCP in regulating neural growth during regeneration in both vertebrates and invertebrates.

Following inhibition of PCP genes, our data demonstrate that excess neural tissue is produced and excess proliferation occurs in planarian regenerates, continuing to arise long after controls have ceased regenerative growth. While the data are consistent with loss of PCP resulting in increased neurons due to increased stem cell progeny, subsequent investigations will specifically delineate the individual contributions of proliferation versus axonal patterning in PCP regulation of neural growth. Similarly, our data show that PCP inhibition leads to ectopic neural differentiation, as illustrated by the appearance of excess eye structures when PCP is lost (Fig. 3). This could reflect a failure to spatially restrict neural differentiation (thus causing photoreceptor cells to occur within the endogenous field as well as ectopically). While our data cannot exclude this hypothesis, any contribution to spatial restriction is probably secondary, since ectopic eye structures were never seen outside of the normal cephalic/head region. Instead, our findings suggest that the major role of PCP during neural regeneration

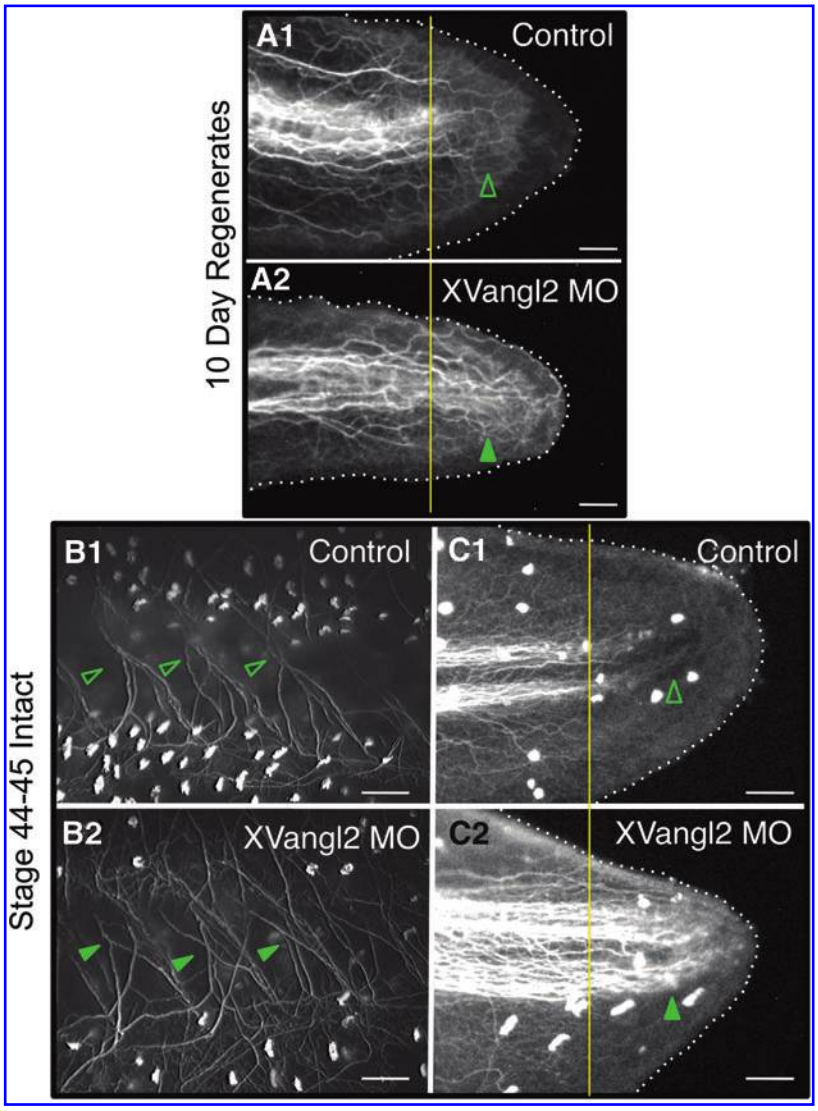

FIG. 6. PCP regulation of neural growth is conserved in vertebrates. Immunofluorescent anti-acetylated-tubulin labeling of *Xenopus* tadpole neurons. **(A)** New tail at 10 days of regeneration. *XVangl2* morpholino (MO)-injected regenerates have 33% more nerve growth toward tail tip ($P < 0.01$, $n \geq 8$). **(B, C)** Stage 44–45 intact embryos. **(B)** Z-stack of motorneurons in flank. **(C)** *XVangl2-MO* results in 21% more nerve growth toward tail tip ($P < 0.001$, $n \geq 13$). *Solid arrowheads*: increased nerve growth. *Open arrowheads*: no nerve growth (or for B1 normal nerve growth). [*Bright spots* in **(B, C)** are ciliary staining.] *Yellow line* aligned to nerve length in control tails. *Dotted lines* represent tail boundaries. Anterior is left. Scale bars: 100 μm. Color images available online at www.liebertonline.com/scd

is to temporally restrict neural differentiation (thus when lost causing neural growth to continue long after neural regeneration should be complete), as illustrated by the gradual appearance of excess pigment cells after regeneration of the primary eyes in PCP-inhibited worms (Fig. 5A).

The data suggest that PCP genes are required to properly terminate neural growth during regeneration, homeostasis, and development—3 instances in which large-scale pattern depends on growth regulation of individual cells. PCP regulation of neural growth during development suggests that planar polarity may play a role in neural plasticity by inhibiting the number of neurons formed during neurogenesis; this model will also be investigated in subsequent studies. In addition to highlighting a mechanism by which (neural) tissue growth is normally stopped, our results indicate that a conserved mechanism stops growth in diverse biological processes. Our data also provide evidence that limiting the extent of neural tissue is in fact an ancestral role of PCP, as *Vangl2* inhibition during *Xenopus* development and tail regeneration also resulted in increased neural growth. Although invertebrates, planarians' similarity to the common bilaterian ancestor suggests that PCP's role in restricting neural growth is conserved throughout the Bilateria. This raises the interesting speculation that this ancestral role for PCP may have been co-opted in non-regenerative organisms during tumorigenesis. This is supported by growing evidence for the involvement of PCP during cancer, from findings such as the tumor suppressor role of Vangl2 [38,39]. Our data show that disrupted PCP signals the formation of new neural tissue and suggests that reestablishing intact PCP halts further neural replacement. In this way, we propose that PCP acts as a sensor by which neural tissue can determine the status of its fine-level organization, signaling "all is complete" when replacement is no longer needed. Finally, our data show that PCP inhibition promotes regeneration, which suggests that pharmacological PCP inhibitors might be a viable approach toward translational therapies.

Acknowledgments

The authors thank L. Vandenberg for help with *Xenopus*, C. Stevenson for molecular assistance, and K. Watanabe and P. Reddien for reagents. W.S.B. also thanks J.L.B. for continued

support. W.S.B. was supported by NIH Kirschstein-NRSA grant F32 GM08354. M.L. gratefully acknowledges support by the Mathers Foundation, as well as NSF grant IBN# 0347295, NHTSA grant DTNH22-06-G-00001, and NIH grant HD055850.

Author Disclosure Statement

No competing financial interests exist.

References

1. Aboobaker AA. (2011). Planarian stem cells: a simple paradigm for regeneration. Trends Cell Biol 21:304–311.
2. Baguna J, E Salo and C Auladell. (1989). Regeneration and pattern formation in planarians. III. Evidence that neoblasts are totipotent stem cells and the cells. Development (Cambridge, England) 107:77–86.
3. Axelrod JD. (2009). Progress and challenges in understanding planar cell polarity signaling. Semin Cell Dev Biol 20:964–971.
4. Ju R, P Cirone, S Lin, H Griesbach, DC Slusarski and CM Crews. (2010). Activation of the planar cell polarity formin DAAM1 leads to inhibition of endothelial cell proliferation, migration, and angiogenesis. Proc Natl Acad Sci U S A 107:6906–6911.
5. Shi J and L Wei. (2007). Rho kinase in the regulation of cell death and survival. Arch Immunol Ther Exp 55:61–75.
6. Sopko R and H McNeill. (2009). The skinny on fat: an enormous cadherin that regulates cell adhesion, tissue growth, and planar cell polarity. Curr Opin Cell Biol 21:717–723.
7. Ciruna B, A Jenny, D Lee, M Mlodzik and AF Schier. (2006). Planar cell polarity signalling couples cell division and morphogenesis during neurulation. Nature 439:220–224.
8. Leong SY, CH Faux, A Turbic, KJ Dixon and AM Turnley. (2010). The Rho kinase pathway regulates mouse adult neural precursor cell migration. Stem cells (Dayton, Ohio) 29:332–343.
9. Tissir F and AM Goffinet. (2010). Planar cell polarity signaling in neural development. Curr Opin Neurobiol 20:572–577.
10. Vivancos V, P Chen, N Spassky, D Qian, A Dabdoub, M Kelley, M Studer and S Guthrie. (2009). Wnt activity guides facial branchiomotor neuron migration, and involves the PCP pathway and JNK and ROCK kinases. Neural Dev 4:7.
11. Almuedo-Castillo M, E Salo and T Adell. (2011). Dishevelled is essential for neural connectivity and planar cell polarity in planarians. Proc Natl Acad Sci U S A 108:2813–2818.
12. Koopowitz H and P Chien. (1974). Ultrastructure of the nerve plexus in flatworms. I. Peripheral organization. Cell Tissue Res 155:337–351.
13. Cebria F. (2008). Organization of the nervous system in the model planarian *Schmidtea mediterranea*: an immunocytochemical study. Neurosci Res 61:375–384.
14. Nishimura K, Y Kitamura, T Taniguchi and K Agata. (2010). Analysis of motor function modulated by cholinergic neurons in planarian Dugesia japonica. Neuroscience 168:18–30.
15. Nishimura K, Y Kitamura, Y Umesono, K Takeuchi, K Takata, T Taniguchi and K Agata. (2008). Identification of glutamic acid decarboxylase gene and distribution of GABAergic nervous system in the planarian Dugesia japonica. Neuroscience 153:1103–1114.
16. Nishimura K, Y Kitamura, T Inoue, Y Umesono, S Sano, K Yoshimoto, M Inden, K Takata, T Taniguchi, S Shimohama and K Agata. (2007). Reconstruction of dopaminergic neural network and locomotion function in planarian regenerates. Dev Neurobiol 67:1059–1078.
17. Gentile L, F Cebria and K Bartscherer. (2011). The planarian flatworm: an *in vivo* model for stem cell biology and nervous system regeneration. Dis Model Mech 4:12–19.
18. Robb SM, E Ross and A Sanchez Alvarado. (2008). SmedGD: the *Schmidtea mediterranea* genome database. Nucleic Acids Res 36:D599–D606.
19. Cebria F and PA Newmark. (2005). Planarian homologs of netrin and netrin receptor are required for proper regeneration of the central nervous system and the maintenance of nervous system architecture. Development (Cambridge, England) 132:3691–3703.
20. Pearson BJ, GT Eisenhoffer, KA Gurley, JC Rink, DE Miller and A Sanchez Alvarado. (2009). Formaldehyde-based whole-mount *in situ* hybridization method for planarians. Dev Dyn 238:443–450.
21. Reddien PW, NJ Oviedo, JR Jennings, JC Jenkin and A Sanchez Alvarado. (2005). SMEDWI-2 is a PIWI-like protein that regulates planarian stem cells. Science (New York, NY) 310:1327–1330.
22. Eisenhoffer GT, H Kang and A Sanchez Alvarado. (2008). Molecular analysis of stem cells and their descendants during cell turnover and regeneration in the planarian *Schmidtea mediterranea*. Cell Stem Cell 3:327–339.
23. Petersen CP and PW Reddien. (2008). Smed-betacatenin-1 is required for anteroposterior blastema polarity in planarian regeneration. Science (New York, NY) 319:327–330.
24. Oviedo NJ, PA Newmark and A Sanchez Alvarado. (2003). Allometric scaling and proportion regulation in the freshwater planarian *Schmidtea mediterranea*. Dev Dyn 226:326–333.
25. Oviedo NJ, CL Nicolas, DS Adams and M Levin. (2008). Gene knockdown in planarians using RNA interference. CSH Protoc 2008:pdb prot5054.
26. Antic D, JL Stubbs, K Suyama, C Kintner, MP Scott and JD Axelrod. (2010). Planar cell polarity enables posterior localization of nodal cilia and left-right axis determination during mouse and *Xenopus* embryogenesis. PLoS One 5:e8999.
27. Mitchell B, JL Stubbs, F Huisman, P Taborek, C Yu and C Kintner. (2009). The PCP pathway instructs the planar orientation of ciliated cells in the *Xenopus* larval skin. Curr Biol 19:924–929.
28. Sive H, R Grainger and Harland RM. (2000). *Early Development of Xenopus laevis: A Laboratory Manual*. Cold Spring Harbor Laboratory Press, Cold Spring Harbor, New York.
29. Sakai F, K Agata, H Orii and K Watanabe. (2000). Organization and regeneration ability of spontaneous supernumerary eyes in planarians—eye regeneration field and pathway selection by optic nerves. Zoolog Sci 17:375–381.
30. Ma C, Y Gao, G Chai, H Su, N Wang, Y Yang, C Li, D Miao and W Wu. (2010). Djrho2 is involved in regeneration of visual nerves in Dugesia japonica. J Genet Genomics 37:713–723.
31. Wenemoser D and PW Reddien. (2011). Planarian regeneration involves distinct stem cell responses to wounds and tissue absence. Dev Biol 344:979–991.
32. Shibata N, L Rouhana and K Agata. (2010). Cellular and molecular dissection of pluripotent adult somatic stem cells in planarians. Dev Growth Differ 52:27–41.
33. Wagner DE, IE Wang and PW Reddien. (2011). Clonogenic neoblasts are pluripotent adult stem cells that underlie planarian regeneration. Science (New York, NY) 332:811–816.

34. Tseng AS, WS Beane, JM Lemire, A Masi and M Levin. (2010). Induction of vertebrate regeneration by a transient sodium current. J Neurosci 30:13192–13200.
35. Slack JM, G Lin and Y Chen. (2008). The *Xenopus* tadpole: a new model for regeneration research. Cell Mol Life Sci 65:54–63.
36. Wallingford JB and RM Harland. (2002). Neural tube closure requires Dishevelled-dependent convergent extension of the midline. Development (Cambridge, England) 129:5815–5825.
37. Park M and RT Moon. (2002). The planar cell-polarity gene stbm regulates cell behaviour and cell fate in vertebrate embryos. Nat Cell Biol 4:20–25.
38. Cantrell VA and JR Jessen. (2010). The planar cell polarity protein Van Gogh-Like 2 regulates tumor cell migration and matrix metalloproteinase-dependent invasion. Cancer Lett 287:54–61.
39. Wang Y. (2009). Wnt/planar cell polarity signaling: a new paradigm for cancer therapy. Mol Cancer Ther 8:2103–2109.

Address correspondence to:
Dr. Michael Levin
Biology Department and Tufts Center for Regenerative and Developmental Biology
Tufts University
200 Boston Avenue, Suite 4600
Medford, MA 02155-4243

E-mail: michael.levin@tufts.edu

Received for publication October 24, 2011
Accepted after revision February 16, 2012
Prepublished on Liebert Instant Online February 16, 2012